Proceedings of Ninth World Conference on Earthquake Engineering
August 2-9, 1988, Tokyo-Kyoto, JAPAN (Vol.VIII)

SI-9

SHAKING TABLE TEST ON 1/7TH-SCALE MODELS OF 11-STORY REINFORCED CONCRETE HIGH-RISE FRAME STRUCTURE WITH WALL COLUMNS

Isamu ABE[1], Tsuneo OKADA[2], Yoshikazu KITAGAWA[3],
Hisahiro HIRAISHI[3], Masafumi SHIN[1], Hiroshi HOSOYA[1]

[1]Tsukuba Research Institute, Okumura Corporation,
Tsukuba-shi, Ibaraki, 300-33 Japan
[2]Institute of Industrial Science, University of Tokyo,
Minato-ku, Tokyo, 106 Japan
[3]Building Research Institute, Ministry of Construction,
Tsukuba-shi, Ibaraki, 305 Japan

SUMMARY

The objectives of this test are to understand the behavior of HFW (High-rise Frame Structure with Wall Columns) during an earthquake, and to verify the compatibility of the analysis with the test results. Two 1/7th scaled 11-story HFW models were tested on the shaking table. One model was excited in the longitudinal direction, and the other in the longitudinal and transverse directions simultaneously. As a result of the test, the one-way test model failed in girder by bending moment, and the two-way test model failed in wall and girder by bending moment. Calculated maximum shear strength in the analysis was close to the experimental result in the longitudinal direction, when half or whole of the transverse bay length was assumed as the effective flange width.

INTRODUCTION

The study on reinforced concrete high-rise frame structure with wall columns has been carried out to develop comfortable apartment houses at a low cost in Japan. It is important problem to secure strength and to keep the ductility under high axial force or the high shear force, especially for high-rise structures. In this study in order to examine the aseismic ability of HFW, the shaking table tests were carried out by using a couple of three-dimensional structural models. The dynamic characteristics of HFW were studied by comparing the response values of the two excitation tests and by comparing the analysis.

OUTLINE OF EXPERIMENTS

Prototype A prototype structure was an 11-story standard type, which consisted of 2 frames with 3 bays in the longitudinal direction and 4 walls with 1 bay in the transverse direction. In accordance with the guidelines for HFW design, the calculated horizontal strength of the prototype structure is 0.34 (in the longitudinal direction = x-dir.), and 0.61 (in the transverse direction = y-dir.) as base shear coefficient. At this time, the models were designed to fail in the girder in the x-dir. and to fail in the wall in the y-dir. by bending moment.

Models An overview of the model is shown in Photo. 1. The plan and the section of the model and the location of instruments are shown in Fig. 1. The law of similarity is shown in Table 1. According to the law of similarity, two 1/7th scaled models were fabricated by microconcrete and scaled deformed bars. One model was used for the one-way test in the x-dir., and the other model was used

for the two-way test in the x-dir. and the y-dir. The similarity ratio of axial stress was 1/2 due to restriction of the capacity of the shaking table.

Material The material properties of microconcrete cured by spray are shown in Table 2. The reinforcing bars consisted of three kinds of scaled deformed bars (D2,D3,D4). The material properties of the reinforcing bars are shown in Table 3. The reinforcing bar arrangement was according to the guidelines for HFW design.

Shaking Table and Input Motion The shaking table is driven in three-dimensional excitation. The capacity of acceleration is 3G for loading up to 20 tons with the maximum stroke of ±125mm. For input excitation for the shaking table tests, the recorded N-S component at Hachinohe Harbour (in the y-dir.) and E-W component (in the x-dir.) obtained during the Tokachi-Oki Earthquake in 1968 were applied. According to the law of similarity, the time axis was scaled to $1/\sqrt{14}$, and the amplitudes were doubled.

EXPERIMENTAL RESULTS

Natural Frequency and Damping Coefficient The loading sequence and the outline of experimental results are shown in Table 4. The relation between the fundamental natural frequency and damping coefficient is shown in Fig. 2. According to the decrease of the natural frequency, the damping coefficients increased.

Failure Mode Final crack patterns are shown in Fig. 3 and the yielding points of reinforcing bars are shown in Fig. 4. Finally, in the one-way test, the lower part of the column of the 1st and 2nd stories failed in combined bending and compression. In the two-way test, after the lower part of the wall of the 1st story failed by bending moment in the y-dir., the lower part of the column of the 1st story failed by compressive stress in the x-dir. The both models failed by bending moment at the end of the girder of almost all stories, and the quantity of cracks of the two-way test was less than that of the one-way test. The reinforcing bars of both models yielded from the early excitation tests, at the lower and upper parts of the columns of the 1st story and at lower part of the columns of the 2nd story.

Maximum Response Distribution The maximum response distribution of inter-story displacement angle in the x-dir. is shown in Fig. 5. In comparing the one-way and two-way tests of which the input maximum accelerations were close (W11 vs. W21, W12 vs. W22, W15 vs. W24), the maximum inter-story displacements of the one-way test were about 1.5~2.0 times as large as those of the two-way test. Due to the fundamental natural period of the one-way test being a little longer than that of the two-way test, the displacement of the one-way test was more amplified by the component of input wave than that of the two-way test. So the response of the model depended on the change of the fundamental period (Fig. 2).

Story Shear Force and Q-δ Curves The maximum story shear force of the 1st story is shown in Table 5, and the story shear force (Q) vs. the inter-story displacement (δ) curve is shown in Fig. 6. The maximum base shear coefficients in the x-dir. of both tests were about 1.5 times as much as the calculated one of the prototype structure. As compared with two Q-δ curves containing the final excitation tests, the ability of deformation of the models were different. For the one-way test, the strength did not decrease at the inter-story displacement angle of about 1/100 (Fig. 8), but for the two-way test, the strength of the 1st story suddenly decreased after the inter-story displacement angle of about 1/130.

ANALYTICAL RESULTS

Analytical Model The structure was represented by the resultant model as shown

in Fig. 7 (Ref.1). The stiffness and strength were calculated by the formulas of the guideline for HFW design. The effective flange width as shown in Table 6 was examined. In the static analysis, five cases (Case A~E) were compared. The distribution of the external force was adopted as the linear one in proportion to the height. In the dynamic analysis, two cases (Case B, C) were compared. For reference, the strength of columns and girders and strength ratio for Case C are shown in Table 7. The modified Degrading Tri-linear model was used for the hysteresis rule (Ref.2). The input earthquake motion was composed of the recorded values on the shaking table.

Static Analysis The analytical results of the Q-δ curve at the 1st story are shown in Fig. 8. In this figure, the marks (● , ■) show the displacement at the time the positive and negative story shear attained the maximum values. For the range of small displacement, Case B, as the deformation becomes large and the crack increases, Case C. And when the maximum shear strength approaches maximum value, Case C, D. Each case is close to the experimental results.

Dynamic Analysis The maximum response distributions of acceleration and relative displacement are shown in Fig. 9. The distributions of the maximum acceleration are close to the experimental result up to W14. At W15 and W16, the analytical responses of upper stories are considerably smaller than the experimental results. However, as to the relative displacement response, Case B is close to the experimental result, and Case C is smaller than the experimental result. This tendency is clear at the upper stories. The Q-δ hysteresis loop at the 1st and 5th stories are shown in Fig. 10. Case C is close to the maximum value of shear force and displacement. However, the displacement to the positive direction is small, and the most outside hysteresis loop is large because the deterioration of the stiffness at the previous excitation is smaller than the test result.

CONCLUSIONS

The important results obtained in this study are summarized as follows:
(1) One-way test model failed in girder by bending moment, and two-way test model failed in wall and girder by bending moment. This tendency corresponded to the assumed collapse mechanism.
(2) The maximum base shear coefficient obtained from tests in the longitudinal direction were about 1.5 times as much as the calculated one of the prototype structure, because of the difference between the test and calculation concerning both the assumed external force distribution and the effective flange width.
(3) The maximum shear strength of static analysis and Q-δ curve of dynamic analysis were close to the experimental results, when half or whole of the transverse bay length was considered as the effective flange width.

ACKNOWLEDGEMENTS

The authors wish to express their appreciation to Mr. T. Kashima, Building Research Institute, Messrs. F. Kumazawa and M. Yamamoto, University of Tokyo, and to Mr. K. Yasui, Okumura Corporation, for their help during the tests.

REFERENCES

1 MASUO, K., Abe, I., and Shin, M., "Analytical study on elasto-plastic deformation behavior of multistory reinforced concrete structures with cantilever shear walls," Transaction of A.I.J., No.339, (1984). (in Japanese)
2 KITAGAWA, Y., and MIDORIKAWA, M., "Dynamic properties and response analysis of a full-scale reinforced concrete seven-story structure - Part of U.S.-JAPAN cooperative research program -," Transaction of A.I.J., No.380, (1987).

Table 1 Law of Similarity

Items	T.S.R.	E.S.R.
Length	1/7	1/7
Area	1/49	1/49
Density	7	7/2
Young's modulus	1	1
Strain	1	1
Stress	1	1
Force	1/49	1/49
Displacement	1/7	1/7
Velocity	$\sqrt{1/7}$	$\sqrt{2/7}$
Acceleration	1	2
Frequency	$\sqrt{7}$	$\sqrt{14}$
Time	$1/\sqrt{7}$	$1/\sqrt{14}$
Axial stress	1	1/2
Displacement angle	1	1
Base shear coefficient	1	2

T.S.R. : Target similarity ratio
E.S.R. : Experiment similarity ratio

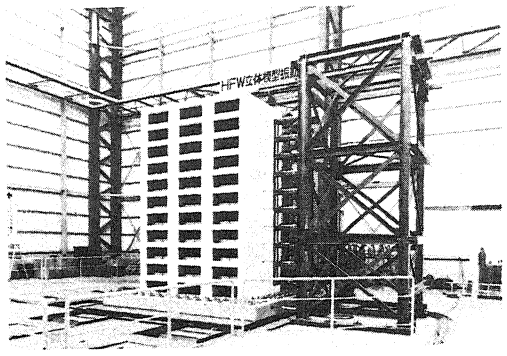

Photo. 1 Overview of Model

Table 2 Microconcrete Material Properties

Model	Compressive strength (kg/cm^2)	Splitting strength (kg/cm^2)	Secant modulus* ($\times 10^5 kg/cm^2$)
one-way	184~262	14.2~24.2	1.76~2.02
tow-way	239~335	19.1~29.3	1.93~2.37

(Standard curing, Age : 28days * at 1/3Fc
Compressive strength = 199 kg/cm^2)

Table 3 Reinforcing Bar Material Properties

Bar	Yield strength (kg/cm^2)	Breaking strength (kg/cm^2)	Breaking stretch (%)	Elastic modulus ($\times 10^6 kg/cm^2$)
D2	4150	4630	10.9	1.59
D3	3500	4450	27.4	2.07
D4	3460	4650	29.4	2.23

Table 4 (1) Response Value

One-way excitation test					
Test no.	Longitudinal direction (x-dir.)				
	A.S.T. (gal)	N.F. (Hz)	D.C. (%)	R.D.A.	I.D.A.
S12	-	5.7	2.9		
W11	+114	-	-	1/1327	1/699
S13	-	5.3	2.7		
W12	+298	-	-	1/440	1/297
W13	-265	-	-	1/336	1/170
S14	-	3.7	2.9		
W14	+368	-	-	1/217	1/133
S15	-	3.0	3.8		
W15	+830	-	-	1/118	1/72
S16	-	2.2	5.2		
W16	+1204	-	-	1/81	1/51
S17	-	1.8	5.6		
W17	+1174	-	-	1/38	1/36
S18	-	1.6	8.4		

Table 5 Maximum Story Shear Force of 1st Story

One-way excitation			Two-way excitation test				
Dir.	x-dir.		Dir.	x-dir.		y-dir.	
Test no.	M.B.S. (ton)	B.S.C.	Test no.	M.B.S. (ton)	B.S.C.	M.B.S. (ton)	B.S.C.
W11	8.6	0.28	W21	8.0	0.26	6.2	0.20
W12	19.0	0.61	W22	19.9	0.64	15.3	0.49
W13	21.9	0.71	W23	22.6	0.73	24.8	0.80
W14	26.5	0.85	W24	31.7	1.02	25.5	0.82
W15	29.3	0.94	W25	34.2	1.10	33.8	1.09
W16	28.5	0.92					

M.B.S. : Maximum base shear
B.S.C. : Base shear coefficient

A.S.T. : Maximum acceleration on shaking table
N.F. : Fundamental natural frequency
D.C. : Fundamental damping coefficient
R.D.A. : Maximum top-level relative displacement angle
I.D.A. : Maximum inter-story displacement angle

Table 4 (2) Response Value

two-way exitation test										
Test no.	Longitudinal direction (x-dir.)					Transverse direction (y-dir.)				
	A.S.T. (gal)	N.F. (Hz)	D.C. (%)	R.D.A.	I.D.A.	A.S.T. (gal)	N.F. (Hz)	T.L. (%)	R.D.A.	I.D.A.
S21	-	7.2	2.9	-	-	-	12.4	2.0	-	-
W21	+96	-	-	1/2006	1/638	+112	-	-	1/4834	1/1745
S22	-	7.2	2.3	-	-	-	12.2	1.8	-	-
W22	-335	-	-	1/682	1/342	+323	-	-	1/2421	1/1040
S23	-	6.3	4.3	-	-	-	11.9	1.8	-	-
W23	+463	-	-	1/444	1/236	+654	-	-	1/1343	1/659
S24	-	5.7	4.3	-	-	-	10.9	2.4	-	-
W24	+762	-	-	1/232	1/163	+779	-	-	1/806	1/628
S25	-	4.2	6.6	-	-	-	10.2	2.3	-	-
W25	+933	-	-	1/98	1/60	+1217	-	-	1/285	1/128
S26	-	3.5	6.8	-	-	-	9.0	3.1	-	-
W26	+889	-	-	-	-	-1018	-	-	-	-
S27	-	2.9	7.5	-	-	-	6.6	3.2	-	-

Wxx : Excitation test to examine the dynamic behavior in earthquake.

Sxx : Excitation test to obtain the natural frequency and damping coefficient.

W11~ W16 Time axis : $1/\sqrt{14}$
W21~ W25
W17, W26 Time axis : $1/\sqrt{7}$

Table 6 Analyzed Cases

Analyzed case	Effective flange width	
	Trans. wall	Slab
Case A	0.0 × hight	0.0 × clear span[3]
Case B	0.1 × hight	0.1 × clear span[3]
Case C	Half width[1]	Half width[1]
Case D	Whole width[2]	Whole width[4]
Case E	Whole width[2]	Whole width[5]

1) Half width of transverse bay length
2) Whole width of transverse bay length
3) Clear span of girder
4) Whole width of transverse bay length (neglect the effect of beam)
5) Whole width of transverse bay length (consider the effect of beam)

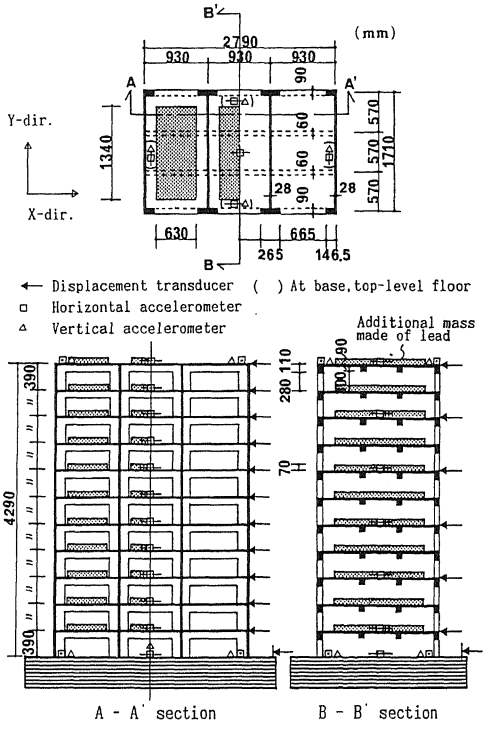

Fig. 1 Plan and Section of Model, Location of Instruments

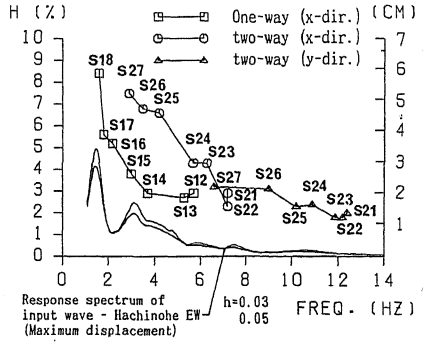

Fig. 2 Transition of Fundamental Natural Frequency and Damping Coefficient

Table 7 Column-Girder Strength Ratio

Case C (ton·m)

F	Column cMy	Girder gMy	Ratio cMy/gMy
11	5.76	4.37	1.32
10	11.72	4.37	2.68
9	12.12	5.10	2.38
8	12.53	5.82	2.15
7	12.93	6.55	1.97
6	13.33	6.55	2.04
5	13.73	6.93	1.98
4	14.13	6.93	2.04
3	14.79	7.66	1.93
2	15.45	7.66	2.02
1	16.01	7.66	2.09

cMy : Total flexural strength of columns at column-girder joints
gMy : Total flexural strength of girders at column-girder joints

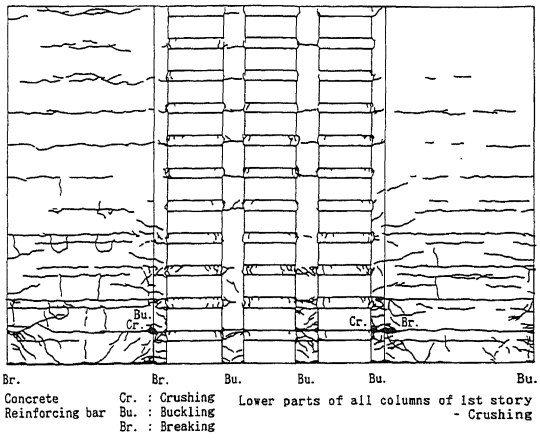

(1) One-way Test (After W17)

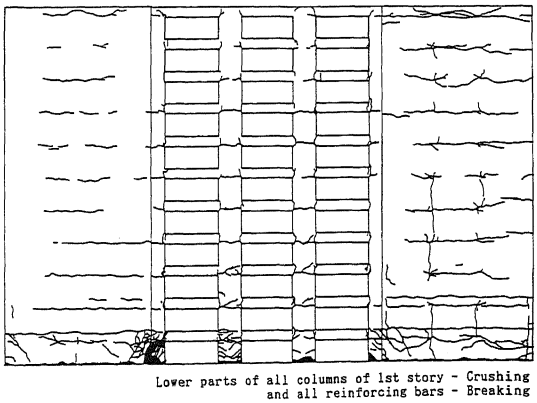

(2) Two-way Test (After W26)

Fig. 3 Final Crack Patterns

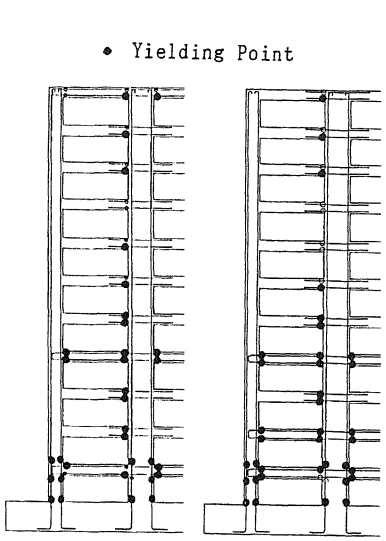

(1) One-way Test (After W17) (2) Two-way Test (After W26)

Fig. 4 Yielding Points of Reinforcing Bar

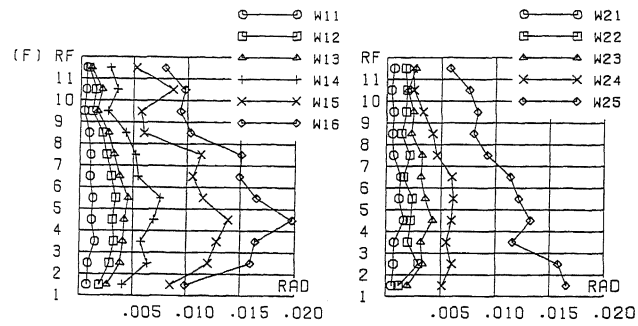

(1) One-way Test (W11~W16) (2) Two-way Test (W21~W25)

Fig. 5 Maximum Response Inter-story Displacement Angle Distribution (X-dir.)

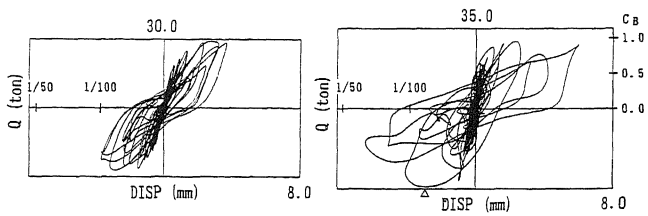

(1) One-way Test (W11~W16) (2) Two-way Test (W21~W25)

Fig. 6 Q - δ Curve (1st Story in X-dir.)

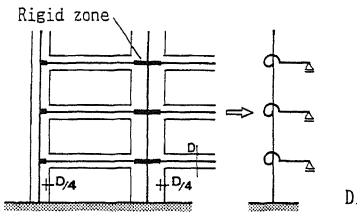

Fig. 7 Analyzed Model

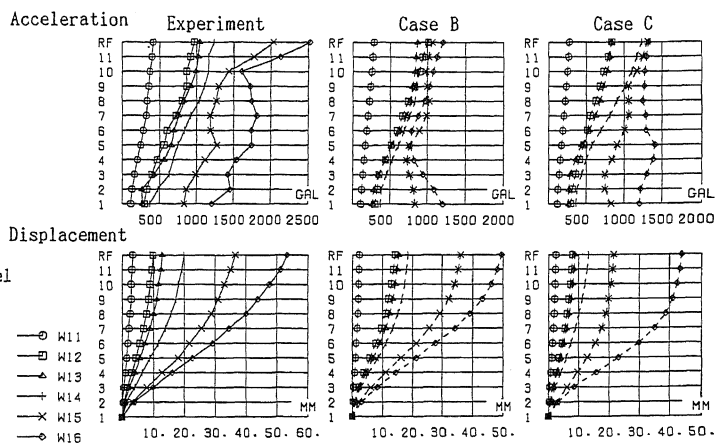

Fig. 9 Maximum Response Distribution (X-dir.)

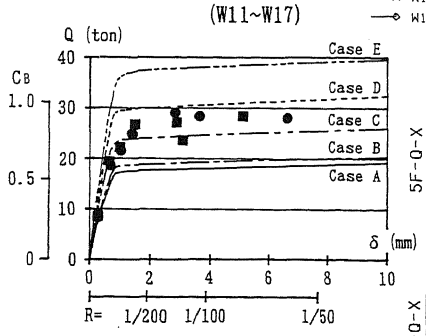

Fig. 8 Q - δ Curve (1st Story in X-dir.)

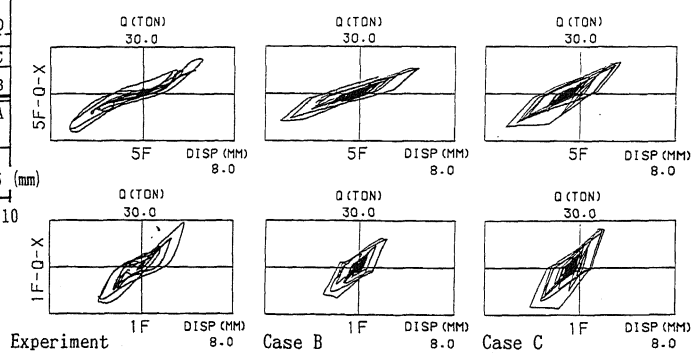

Fig. 10 Q-δ Curve (W16 - One-way Test)